Schwarzschild-Finsler-Randers spacetime: Dynamical analysis, Geodesics and Deflection Angle

Schwarzschild-Finsler-Randers spacetime: Geodesics, Dynamical Analysis and Deflection Angle

E. Kapsabelis,[1,*] P. G. Kevrekidis,[2,†] P. C. Stavrinos,[3,‡] and A. Triantafyllopoulos[1,§]

[1]*Section of Astrophysics, Astronomy and Mechanics, Department of Physics, National and Kapodistrian University of Athens, Panepistimiopolis 15784, Athens, Greece*

[2]*Department of Mathematics and Statistics, University of Massachusetts, Amherst, MA 01003-9305, USA*

[3]*Department of Mathematics, National and Kapodistrian University of Athens, Panepistimiopolis 15784, Athens, Greece*

In this work, we extend the study of Schwarzschild-Finsler-Randers (SFR) spacetime previously investigated by a subset of the present authors [1, 2]. We will examine the dynamical analysis of geodesics which provides the derivation of the energy and the angular momentum of a particle moving along a geodesic of SFR spacetime. This study allows us to compare our model with the corresponding of general relativity (GR). In addition, the effective potential of SFR model is examined and it is compared with the effective potential of GR. The phase portraits generated by these effective potentials are also compared. Finally, we deal with the derivation of the deflection angle of the SFR spacetime and we find that there is a small perturbation from the deflection angle of GR. It comes from the anisotropic metric structure of the model and especially from a Randers term which provides a small deviation from GR.

I. INTRODUCTION

Einstein's field equations in general relativity predict that the curvature is produced not only by the distribution of mass-energy but also by its motion [3]. Candidate metric geometries that can intrinsically describe the motion are the Finsler and Finsler-like geometries which constitute metrical generalizations of Riemannian geometry and depend on position and velocity/momentum/scalar coordinates. These are dynamic geometries that can describe locally anisotropic phenomena and Lorentz violations [4–14] as well as with field equations, FRW and Raychaudhuri equations, geodesics, dark matter and dark energy effects [15–20]. By considering this approach, the gravitational field is interpreted as the metric of a generalized spacetime and constitutes a force-field which contains the motion. This possibility reveals the Finslerian geometrical character of spacetime.

In the framework of applications of Finsler geometry, many works in different directions of geometrical and physical structures have contributed to the extension of research for theoretical and observational approaches during the last years. We cite some works from the literature of the applications of Finsler geometry [6, 7, 12, 20–30].

In the first period of development of applications of Finsler geometry to Physics, especially to General Relativity, remarkable works were published by G. Randers [31], J. I. Horvath [32] and A. Moor [33]. Later, Einstein's field equations were formulated in the Finslerian framework by the works of J. I. Horvath [32, 33], Y. Takano [34] and S. Ikeda [35]. In these studies, the field equations had been considered without calculus of variations. G. S. Asanov [36] explored the Finslerian gravitational field by using Riemannian osculating methods and derived Einstein

* manoliskapsabelis@yahoo.gr
† kevrekid@umass.edu
‡ pstavrin@math.uoa.gr
§ alktrian@phys.uoa.gr

field equations using the variational principle. A class of Finsler spaces (FR standing for Finsler-Randers) originated by G. Randers [31] who studied the physical properties of spacetime with an asymmetrical metric which provides the uni-direction of time-like intervals. This consideration gives a particular interest in a generalized metric structure of the Riemannian spacetime. Based on this form of spacetime, it is possible to investigate the gravitational field with more degrees of freedom in the framework of a tangent/vector/scalar bundle [30, 37, 38]. The FR cosmological model was first introduced in [39, 40]. It is of special interest since the Friedmann equations include an extra geometrical term that acts as a dark energy-fluid. The Finsler-Randers-type spacetime can be considered as a direction-dependent motion of the Riemannian/FRW model.

The local anisotropic structure of spacetime affects the gravitational field and leads to modified cosmological considerations. Based on Finsler or Finsler-like cosmologies, the Friedmann equations include extra terms which influence the cosmological evolution [16, 19, 30, 37]. When Lorentz symmetry holds, the spacetime is isotropic in the sense that all directions and uniform motions are equivalent. The introduction of a vector field in the structure of spacetime causes relativity violations and local anisotropy which arise from breaking the Lorentz symmetry and which affect the metric, curvature, geodesics and null cone [41–48].

An FR space has a metric function of the form

$$F(x,y) = (-a_{\mu\nu}(x)y^{\mu}y^{\nu})^{1/2} + u_{\alpha}y^{\alpha} \tag{1}$$

where u_α is a covector with $||u_\alpha|| \ll 1$, $y^\alpha = \frac{dx^\alpha}{d\tau}$ and $a_{\mu\nu}(x)$ is a Riemannian metric for which the Lorentzian signature $(-,+,+,+)$ has been assumed and the indices μ,ν,α take the values $0,1,2,3$. The geodesics of this space can be produced by (1) and the Euler-Lagrange equations. If u_α denotes a force field f_α and y^α is substituted with dx^α then $f_\alpha dx^\alpha$ represents the spacetime effective energy produced by the anisotropic force field f_α, therefore equation (1) is written as

$$F(x,dx) = \left(-a_{\mu\nu}(x)dx^{\mu}dx^{\nu}\right)^{1/2} + f_{\alpha}dx^{\alpha} \tag{2}$$

This form of metric provides a dynamical effective structure of spacetime. A small differentiation is presented between GR and the FR gravitation model. This is because of the work provided by the one-form A_γ which gives an external motion to the Riemannian spacetime. This motion is an internal concept for the FR spacetime.

A cosmological model can be considered by Eq. (2) if we assume the FRW cosmological metric instead of the general type of the Riemannian one [39, 40]. In this case, we get a Friedmann-Finsler-Randers cosmological model in the following form

$$a_{\mu\nu}(x) = \mathrm{diag}\left[-1, \frac{a^2}{1-\kappa r^2}, a^2r^2, a^2r^2\sin^2\theta\right] \tag{3}$$

This model was also further studied later in [8, 20, 49–65].

In the present paper, we continue the investigation of the Schwarzschild-Finsler-Randers spacetime (SFR) which has been studied in previous works by a subset of the present authors [1, 2]. The structure of the model is given in Section II. In this framework, the geodesics are studied and a dynamical analysis is presented in Section III. We also compare our results with GR and discuss the corresponding similarities and differences. A dynamical analysis for the effective potential of this spacetime is provided in the Section IV, where upon suitable assumptions, the phase portraits of both models (SFR and GR) are presented. The deflection angle of the SFR spacetime is investigated in Section V. Finally, the conclusions of our study and some possible directions for future exploration are presented in Section VI.

II. BASIC STRUCTURE OF THE MODEL

In this section, we briefly present the underlying geometry of the SFR gravitational model, as well as the field equations for the SFR metric. The solution of these equations for this metric is presented at the end of the section. An extended study of this model can be found in [1, 38]. The Lorentz tangent bundle TM is a fibered 8-dimensional manifold with local coordinates $\{x^\mu, y^\alpha\}$ where the indices of the x variables are $\kappa, \lambda, \mu, \nu, \ldots = 0, \ldots, 3$ and the indices of the y variables are $\alpha, \beta, \ldots, \theta = 4, \ldots, 7$. The tangent space at a point of TM is spanned by the so-called adapted basis $\{E_A\} = \{\delta_\mu, \dot{\partial}_\alpha\}$ with

$$\delta_\mu = \frac{\delta}{\delta x^\mu} = \frac{\partial}{\partial x^\mu} - N^\alpha_\mu(x, y)\frac{\partial}{\partial y^\alpha} \tag{4}$$

and

$$\dot{\partial}_\alpha = \frac{\partial}{\partial y^\alpha} \tag{5}$$

where N^α_μ are the components of a nonlinear connection $N = N^\alpha_\mu(x, y)\, \mathrm{d}x^\mu \otimes \dot{\partial}_\alpha$.

The nonlinear connection induces a split of the total space TTM into a horizontal distribution $T_H TM$ and a vertical distribution $T_V TM$. The above-mentioned split is expressed with the Whitney sum:

$$TTM = T_H TM \oplus T_V TM \tag{6}$$

The anholonomy coefficients of the nonlinear connection are defined as

$$\Omega^\alpha_{\nu\kappa} = \frac{\delta N^\alpha_\nu}{\delta x^\kappa} - \frac{\delta N^\alpha_\kappa}{\delta x^\nu} \tag{7}$$

A Sasaki-type metric [66, 67] $\mathcal{G}$ on TM is:

$$\mathcal{G} = g_{\mu\nu}(x, y)\, \mathrm{d}x^\mu \otimes \mathrm{d}x^\nu + v_{\alpha\beta}(x, y)\, \delta y^\alpha \otimes \delta y^\beta \tag{8}$$

where we have defined the metrics $g_{\mu\nu}$ and $v_{\alpha\beta}$ to be pseudo-Finslerian.

A pseudo-Finslerian metric $f_{\alpha\beta}(x, y)$ is defined as one that has a Lorentzian signature of $(-, +, +, +)$ and that also obeys the following form:

$$f_{\alpha\beta}(x, y) = \pm\frac{1}{2}\frac{\partial^2 F^2}{\partial y^\alpha \partial y^\beta} \tag{9}$$

where the function F satisfies the following conditions [66]:

1. F is continuous on TM and smooth on $\widetilde{TM} \equiv TM \setminus \{0\}$, i.e., the tangent bundle minus the null set $\{(x, y) \in TM | F(x, y) = 0\}$.
2. F is positively homogeneous of first degree on its second argument:
$$F(x^\mu, ky^\alpha) = kF(x^\mu, y^\alpha), \qquad k > 0 \tag{10}$$
3. The form
$$f_{\alpha\beta}(x, y) = \frac{1}{2}\frac{\partial^2 F^2}{\partial y^\alpha \partial y^\beta} \tag{11}$$
defines a non-degenerate matrix:
$$\det\left[f_{\alpha\beta}\right] \neq 0 \tag{12}$$

where the plus-minus sign in (9) is chosen so that the metric has the correct signature.

In this work, we will follow the model presented in [1]. The metric $g_{\mu\nu}$ is the classic Schwarzschild one:

$$g_{\mu\nu}\mathrm{d}x^{\mu}\mathrm{d}x^{\nu} = -f dt^2 + \frac{dr^2}{f} + r^2 d\theta^2 + r^2 \sin^2\theta\, d\phi^2 \tag{13}$$

with $f = 1 - \frac{R_s}{r}$ and $R_s = 2GM$ the Schwarzschild radius (we assume units where the speed of light $c = 1$).

Hereafter, we consider an α-Randers type metric as the one in rel.(1) which is distinguished from the β-Randers type metric that is investigated in the Standard Model Extension (SME) [6, 7, 10, 44].

The metric $v_{\alpha\beta}$ is derived from a metric function F_v of the α-Randers type:

$$F_v = \sqrt{-g_{\alpha\beta}(x)y^{\alpha}y^{\beta}} + A_{\gamma}(x)y^{\gamma} \tag{14}$$

where $g_{\alpha\beta} = g_{\mu\nu}\tilde{\delta}^{\mu}_{\alpha}\tilde{\delta}^{\nu}_{\beta}$ is the Schwarzschild metric from Eq. (13) and $A_{\gamma}(x)$ is a covector which expresses a deviation from general relativity, with $|A_{\gamma}(x)| \ll 1$, i.e., we assume that that deviation is small. We choose a non-linear connection with the following form:

$$N^{\alpha}_{\mu} = \frac{1}{2}y^{\beta}g^{\alpha\gamma}\partial_{\mu}g_{\beta\gamma} \tag{15}$$

The metric tensor $v_{\alpha\beta}$ of (14) is derived from (9) after omitting higher order terms $O(A^2)$:

$$v_{\alpha\beta}(x,y) = g_{\alpha\beta}(x) + h_{\alpha\beta}(x,y), \tag{16}$$

where

$$h_{\alpha\beta} = \frac{1}{\tilde{a}}(A_{\beta}g_{\alpha\gamma}y^{\gamma} + A_{\gamma}g_{\alpha\beta}y^{\gamma} + A_{\alpha}g_{\beta\gamma}y^{\gamma}) + \frac{1}{\tilde{a}^3}A_{\gamma}g_{\alpha\epsilon}g_{\beta\delta}y^{\gamma}y^{\delta}y^{\epsilon} \tag{17}$$

with $\tilde{a} = \sqrt{-g_{\alpha\beta}y^{\alpha}y^{\beta}}$. The total metric defined in the previous steps is called the *Schwarzschild-Finsler-Randers* (SFR) metric. As we can see, the term $h_{\alpha\beta}(x,y)$ can be considered as a perturbation of the Schwarzschild metric since $|A_{\gamma}(x)| \ll 1$.

The nonzero coefficients of a canonical and distinguished $d-$connection $\mathcal{D}$ on TM are:

$$L^{\mu}_{\nu\kappa} = \frac{1}{2}g^{\mu\rho}\left(\delta_k g_{\rho\nu} + \delta_{\nu}g_{\rho\kappa} - \delta_{\rho}g_{\nu\kappa}\right) \tag{18}$$

$$L^{\alpha}_{\beta\kappa} = \dot{\partial}_{\beta}N^{\alpha}_{\kappa} + \frac{1}{2}v^{\alpha\gamma}\left(\delta_{\kappa}v_{\beta\gamma} - v_{\delta\gamma}\,\dot{\partial}_{\beta}N^{\delta}_{\kappa} - v_{\beta\delta}\,\dot{\partial}_{\gamma}N^{\delta}_{\kappa}\right) \tag{19}$$

$$C^{\mu}_{\nu\gamma} = \frac{1}{2}g^{\mu\rho}\dot{\partial}_{\gamma}g_{\rho\nu} \tag{20}$$

$$C^{\alpha}_{\beta\gamma} = \frac{1}{2}v^{\alpha\delta}\left(\dot{\partial}_{\gamma}v_{\delta\beta} + \dot{\partial}_{\beta}v_{\delta\gamma} - \dot{\partial}_{\delta}v_{\beta\gamma}\right). \tag{21}$$

See Appendix A for more details.

The field equations for our model have been derived in previous works and can be found in Appendix B. Solving the field equations (B3), (B4) and (B5) to first order in $A_{\gamma}(x)$ in vacuum ($T_{\mu\nu} = Y_{\alpha\beta} = \mathcal{Z}^{\kappa}_{\alpha} = 0$), we get [1]:

$$A_{\gamma}(x) = \left[\tilde{A}_0\left(1 - \frac{R_S}{r}\right)^{1/2}, 0, 0, 0\right] = \left[\tilde{A}_0 f^{1/2}, 0, 0, 0\right] \tag{22}$$

with $\tilde{A}_0$ a constant. While this is an approximate solution, it will be sufficient for our purposes given the assumption $|A_{\gamma}(x)| \ll 1$.

III. GEODESICS

In this section, we will study the geodesics of the SFR and perform a dynamical analysis. We compare our results with the corresponding ones of GR. From the definition of the metric function (14) we have:

$$F(x,dx) = \left(-g_{\mu\nu}(x)dx^\mu dx^\nu\right)^{1/2} + A_\gamma(x)dx^\gamma \tag{23}$$

where $g_{\mu\nu}(x)$ is the Schwarzschild metric and $A_\gamma(x)$ is a one-form vector field with $|A_\gamma(x)| \ll 1$.

By using Eq. (13) and Eq. (23) is written as:

$$F(x,dx) = \left[f dt^2 - \frac{dr^2}{f} - r^2 d\theta^2 - r^2 \sin^2\theta\, d\phi^2\right]^{1/2} + A_\gamma(x)dx^\gamma. \tag{24}$$

We define the Lagrangian

$$L(x,\dot{x}) = F(x,\dot{x}) = \left[f\dot{t}^2 - \frac{\dot{r}^2}{f} - r^2\dot{\theta}^2 - r^2 sin^2\theta\dot{\phi}^2\right]^{1/2} + \tilde{A}_0 f^{1/2}\dot{t}, \tag{25}$$

where we have used Eqs. (24) and (22). From the Euler-Lagrange equations

$$\frac{d}{d\tau}\frac{\partial L}{\partial \dot{x}^\mu} = \frac{\partial L}{\partial x^\mu} \tag{26}$$

we find the equations for the geodesics:

$$\ddot{x}^\lambda + \Gamma^\lambda_{\mu\nu}\dot{x}^\mu\dot{x}^\nu + g^{\kappa\lambda}\Phi_{\kappa\mu}\dot{x}^\mu = 0, \tag{27}$$

where $\Gamma^\lambda_{\mu\nu}$ are the Christoffel symbols of Riemann geometry, $\Phi_{\kappa\mu} = \partial_\kappa A_\mu - \partial_\mu A_\kappa$ and A_μ is the solution from Eq. (22). We notice that from the definition of $\Phi_{\kappa\mu}$ we get a rotation form of geodesics. If A_μ is a gradient of a scalar field, $A_\mu = \dfrac{\partial\Phi}{\partial x^\mu}$ then $\Phi_{\kappa\mu} = 0$ and the geodesics of our model are identified with the Riemmanian ones.

The geodesics of our model can then be explicitly written in the form:

$$\ddot{t} + \frac{1-f}{rf}\dot{r}\dot{t} = -\tilde{A}_0\dot{r}\frac{f^{-3/2}(1-f)}{2r} \tag{28}$$

$$\ddot{r} + \frac{f(1-f)}{2r}\dot{t}^2 - \frac{1-f}{2rf}\dot{r}^2 - rf\left(\dot{\theta}^2 + \sin^2\theta\dot{\phi}^2\right) = -\tilde{A}_0\dot{t}\frac{f^{1/2}(1-f)}{2r} \tag{29}$$

$$\ddot{\theta} + \frac{2}{r}\dot{\theta}\dot{r} - \frac{1}{2}\sin 2\theta\,\dot{\phi}^2 = 0 \tag{30}$$

$$\ddot{\phi} + \frac{2}{r}\dot{\phi}\dot{r} + 2\cot\theta\,\dot{\theta}\dot{\phi} = 0 \tag{31}$$

From the relations (28)-(31) we notice that the first two dynamical equations involve a contribution of extra terms particular to the SFR spacetime while the last two relations are the same as in GR.

We now make a key assumption regarding the angular dependence of the model. Namely, by using $\theta = \frac{\pi}{2}$ we notice that Eq. (30) is satisfied and equations (28), (29) and (31) can be written as:

$$\ddot{t} + \frac{1-f}{rf}\dot{r}\dot{t} = -\tilde{A}_0\dot{r}\frac{f^{-3/2}(1-f)}{2r} \tag{32}$$

$$\ddot{r} + \frac{f(1-f)}{2r}\dot{t}^2 - \frac{1-f}{2rf}\dot{r}^2 - rf\dot{\phi}^2 = -\tilde{A}_0\dot{t}\frac{f^{1/2}(1-f)}{2r} \tag{33}$$

$$\ddot{\phi} + \frac{2}{r}\dot{\phi}\dot{r} = 0 \tag{34}$$

From Eq.(34) we find:

$$r^2\dot{\phi} = J = const. \tag{35}$$

where J is the angular momentum and the relevant equation represents its conservation law. If we use the relation $f' = \frac{1-f}{r}$ where $f = 1 - \frac{2GM}{r}$ and the Leibniz chain-rule $\frac{d}{d\tau} = \frac{dr}{d\tau}\frac{d}{dr} = \dot{r}\frac{d}{dr}$, then Eq. (32) can be written as:

$$f\ddot{t} + \frac{df}{d\tau}\dot{t} = -\tilde{A}_0\frac{df^{1/2}}{d\tau} \tag{36}$$

which, in turn, gives us

$$f\dot{t} + \tilde{A}_0 f^{1/2} = \mathcal{E}_R = const. \tag{37}$$

where $\mathcal{E}_R$ is the energy of the particle moving along the geodesic. We notice that the first term constitutes the energy for a particle moving along the geodesics in general relativity, $E_{GR} = f\dot{t}$ and we can rewrite the relevant expression as:

$$E_{GR} + \tilde{A}_0 f^{1/2} = \mathcal{E}_R. \tag{38}$$

By using Eq. (33) with (35), and (37), we arrive at the (effectively one-degree-of-freedom) radial equation:

$$\ddot{r} + \frac{1-f}{2rf}(\mathcal{E}_R^2 - \dot{r}^2) - \frac{fJ^2}{r^3} = \tilde{A}_0\mathcal{E}_R\frac{f^{-1/2}(1-f)}{2r} \tag{39}$$

where we omitted $O(\tilde{A}_0^2)$ terms. As before, we use the relation $f' = \frac{1-f}{r}$ in (39) to bring it to the equivalent form:

$$\ddot{r} + \frac{f'}{2f}(\mathcal{E}_R^2 - \dot{r}^2) - \frac{fJ^2}{r^3} = \frac{\tilde{A}_0\mathcal{E}_R}{2}f^{-1/2}f' \tag{40}$$

We can further simplify the Eq. (40) by using the Leibniz chain-rule $\frac{d}{d\tau} = \frac{dr}{d\tau}\frac{d}{dr} = \dot{r}\frac{d}{dr}$ and upon deriving the first integral of the motion, we obtain:

$$\dot{r}^2 + f\left(\frac{J^2}{r^2} + \epsilon\right) + 2\tilde{A}_0\mathcal{E}_R f^{1/2} = \mathcal{E}_R^2 \tag{41}$$

where ϵ is a constant and for $\epsilon = 0$ we have null geodesics. The first two terms from (41) constitute the total energy in general relativity (GR), $\mathcal{E}_{GR}^2 = \dot{r}^2 + f(\frac{J^2}{r^2} + \epsilon)$ and the third term emerges from the structure of SFR spacetime and its energetic contribution. Therefore Eq. (41) can be written as:

$$\mathcal{E}_{GR}^2 + 2\tilde{A}_0\mathcal{E}_R f^{1/2} = \mathcal{E}_R^2 \tag{42}$$

Eq. (42) shows that the term $A_\gamma(x)$ from (22) provides an additional energy contribution to the system of GR. Below, we give the Figures 1a, 1b and Fig. 2 for the geodesics of GR and SFR we have obtained by solving the equations (28)-(31). The relevant ordinary differential equations are solved via a standard solver within Mathematica and (r, ϕ) are presented as a function of τ, while Fig. 2 presents the evolution in the original (x, y) plane. In our case, we assume $R_s = 2$ and initial radial distance $r_0 = 3$, so the photons are found on the photonsphere with $r_{ph} = \frac{3}{2}R_s = 3$ in the GR case. The deviation between the trajectories of the SFR and those of the GR is clearly discernible in both figures.

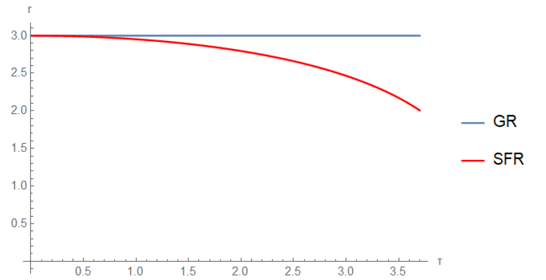

(a) This is an $(\tau$,r) graph for the geodesics of photons for angular momentum $J = 4$ and initial radial distance $r_0 = 3$. The red line shows the SFR geodesics and the blue line the GR geodesics.

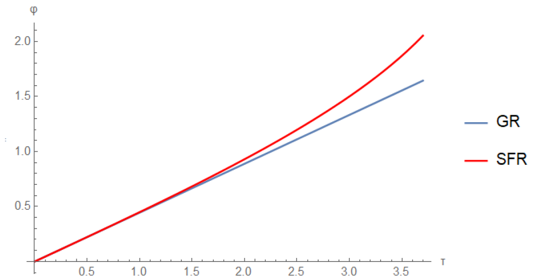

(b) This is an (τ, ϕ) graph for the geodesics of photons for angular momentum $J = 4$ and initial radial distance $r_0 = 3$. The red line shows the SFR geodesics and the blue line the GR geodesics.

From Fig. 1a, we can see that the radial component in the SFR model takes lower values compared to the GR one which remains constant. This difference between the r-components of SFR and GR can be interpreted as the increase of the radius of the photonsphere due to the one-form A_γ as we have shown in [2]. This leads the orbit of the photon to fall inside the event horizon because the initial distance $r_0 = 3$ and energy are not sufficient to allow circular orbits of the photonsphere. That means for an orbit with r constant in the SFR model, the particle needs more energy compared to the GR case. In Fig. 2, the geodesics of GR and SFR are depicted. In the case of GR, the photons move in circular orbits around the black hole. In the SFR model, the photons follow a spiral orbit and fall inside the event horizon.

It is important to remind the reader here that underlying these results is the key assumption of $\theta = \frac{\pi}{2}$ which allows the reduction of the model to an *effective single degree-of-freedom system*. It is important in future work to consider how deviations from this equilibrium value (and the corresponding incorporation of the full dynamical system) may affect the conclusions presented above. However, as the latter is outside the scope of the present study, we now focus on the further analysis of the effective potential of the SFR model and its implications for the phase portrait of the relevant system.

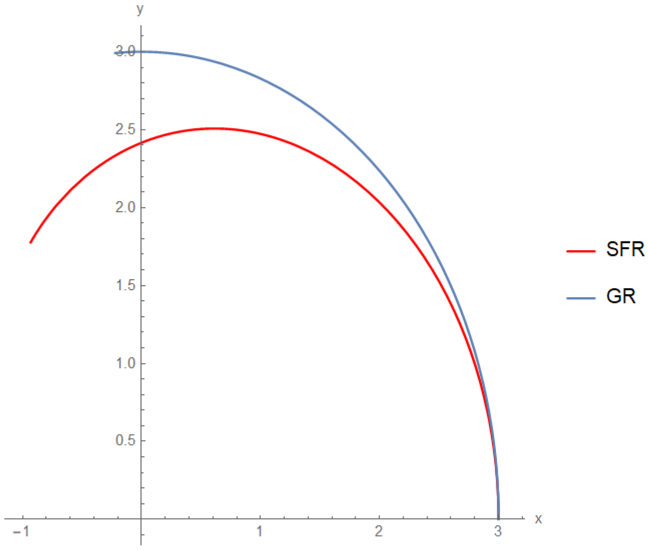

Fig. 2: This is an x-y graph for the geodesics of photons for angular momentum $J = 4$ and initial radial distance $r_0 = 3$. The red line shows the SFR geodesics and the blue line the GR geodesics.

IV. EFFECTIVE POTENTIAL OF SFR MODEL

In this section, we will study the effective potential of the SFR model and compare it with the effective potential of GR. The equation of the energy in GR reads:

$$\dot{r}^2 + f\left(\frac{J^2}{r^2} + \epsilon\right) = \mathcal{E}_{GR}^2 \tag{43}$$

We see from (43) that the effective potential energy landscape is given by:

$$V_{eff,GR} = \frac{1}{2} f\left(\frac{J^2}{r^2} + \epsilon\right) \tag{44}$$

In Fig.3, we show the graph for the effective potential in GR for angular momentum $J = 3, J = 4$ and $J = 5$ to examine its variation for different values of the angular momentum.

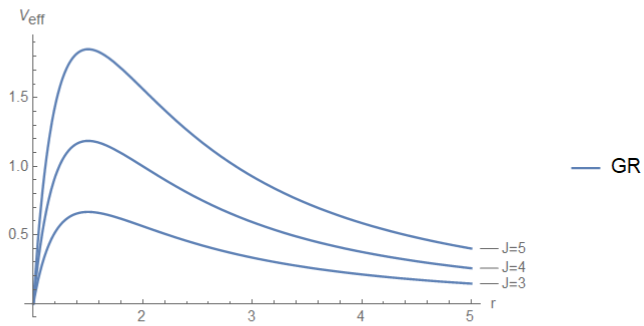

Fig. 3: Graph for the $V_{eff}(r)$ in the GR model for angular momentum $J = 3, J = 4$ and $J = 5$.

We now recall the key difference (and associated additional contribution) to the energetics of the SFR model. In particular, the energy equation for the latter, derived from Eq. (40), is given as:

$$\dot{r}^2 + f\left(\frac{J^2}{r^2} + \epsilon\right) + 2\tilde{A}_0\mathcal{E}_R f^{1/2} = \mathcal{E}_R^2 \tag{45}$$

In (45) the effective potential can be written in the form

$$V_{eff,SFR} = \frac{1}{2}f\left(\frac{J^2}{r^2} + \epsilon\right) + \tilde{A}_0\mathcal{E}_R f^{1/2} \tag{46}$$

The graph for the effective potential in the SFR model (V_{eff}, r) is depicted in Fig. 4, in this case for different values of angular momentum.

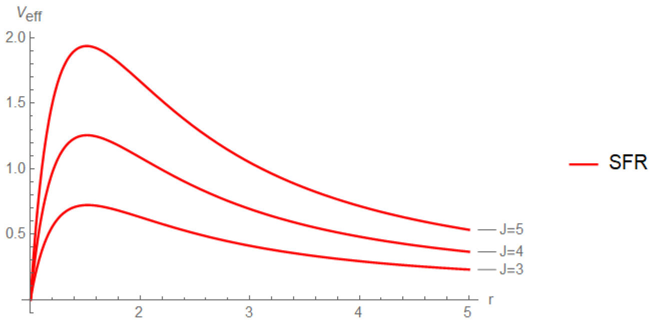

Fig. 4: Graph for the $V_{eff}(r)$ in the SFR model for angular momentum $J = 3$, $J = 4$ and $J = 5$.

In Fig. 5a and 5b we show the effective potentials of the SFR and GR models comparing the two for $J = 1$ and $J = 5$. As we can see in Fig. 5a, the difference between GR and SFR is bigger than that of Fig. 5b. Notably, when the contribution of the angular momentum is weaker, the difference between the two models is more substantial/clearly discernible. When the angular momentum becomes large, the relevant difference is rather weak and the V_{eff} of the two models become proximal.

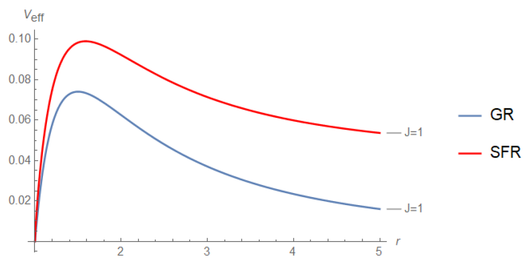

(a) Graph for the $V_{eff}(r)$ in GR (blue line) and SFR (red line) for angular momentum $J = 1$.

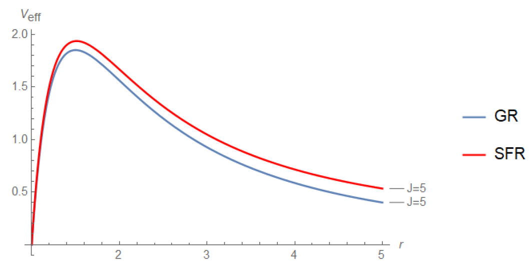

(b) This is a graph for the $V_{eff}(r)$ in GR (blue line) and SFR (red line) for angular momentum $J = 5$.

In Figs. 6a-6b and also 7, we observe the phase portraits associated with the effective potentials depicted above. These phase portraits reflect the existence of an energy barrier whose precise height depends on the value of the angular momentum. Energies below this barrier height result in reflection from the outside and trapping from the inside. On the other hand, energies higher than those of the barrier result in reaching the Schwarzschild radius (if the particle is coming from the outside) or reaching infinity (if the particle is moving outward from the inside). The latter figure demonstrates the differences between the two phase portraits which are quantitative but not qualitative.

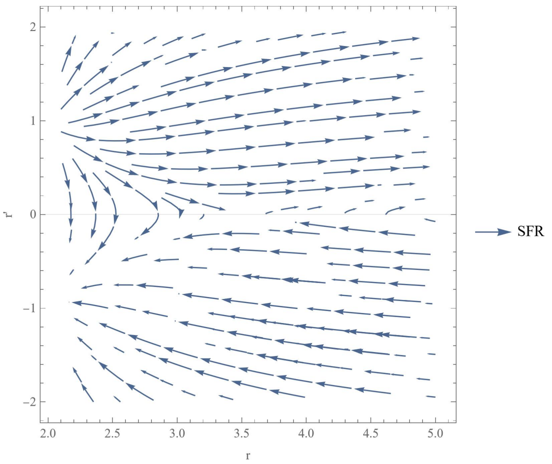

(a) This is a phase plot for the radial geodesics of SFR, representing the trajectories in $(r, \dot{r})$ space.

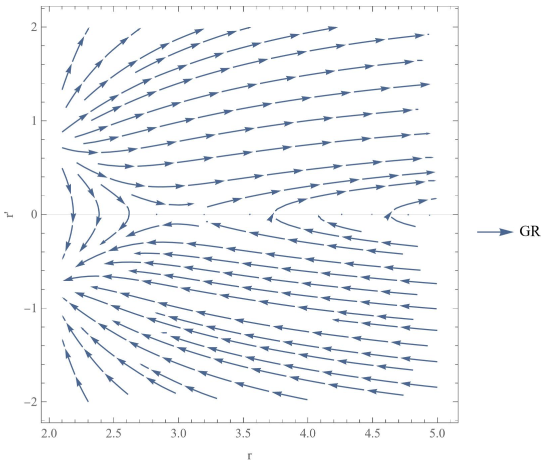

(b) This is a phase plot for the radial geodesics of GR representing the trajectories in $(r, \dot{r})$ space.

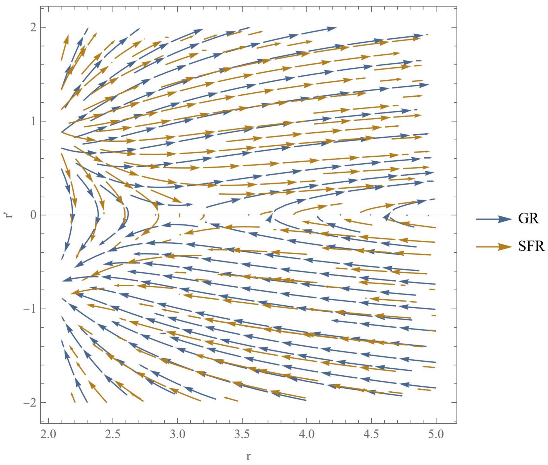

Fig. 7: This is a comparison between the radial phase portraits of the GR (blue) and SFR (yellow) models.

V. DEFLECTION ANGLE

In this section, we will deal with the deflection angle of the SFR model and we will compare our findings with the corresponding ones of the GR model. In this consideration, we take into account photons that pass close to a central mass M. From Eq. (41) for photons, we put $\epsilon = 0$ and we get:

$$\frac{\dot{r}^2}{J^2} + \frac{f}{r^2} + \frac{2\tilde{A}_0 f^{1/2}}{Jb} = \frac{1}{b^2} \tag{47}$$

where $b = J/\mathcal{E}_R$.
By using the Leibniz chain-rule $\dot{\phi} = \frac{d\phi}{d\tau} = \frac{d\phi}{dr}\frac{dr}{d\tau} = \frac{d\phi}{dr}\dot{r}$ with the relations (35) and (47) we have:

$$\frac{\dot{r}^2}{\dot{\phi}^2} = r^4\left(\frac{1}{b^2} - \frac{f}{r^2} - \frac{2\tilde{A}_0 f^{1/2}}{Jb}\right) \tag{48}$$

After some rearrangements we find:

$$\frac{d\phi}{dr} = \frac{1}{r^2}\left(\frac{1}{b^2} - \frac{f}{r^2} - \frac{2\tilde{A}_0 f^{1/2}}{Jb}\right)^{-1/2} \tag{49}$$

The deflection angle is calculated by the integration of (49):

$$\Delta\phi_{SFR} = 2\int_{r_1}^{\infty}\frac{dr}{r^2}\left[\frac{1}{b^2} - \frac{1}{r^2}\left(1 - \frac{2GM}{r}\right) - \frac{2\tilde{A}_0}{Jb}\left(1 - \frac{2GM}{r}\right)^{1/2}\right]^{-1/2} \tag{50}$$

where we have used $f = 1 - \frac{2GM}{r}$.
We perform a change of variables in the integral of Eq. (50):

$$\Delta\phi_{SFR} = 2\int_{0}^{w_1} dw\left[1 - w^2\left(1 - \frac{2GM}{b}w\right) - 2a\left(1 - \frac{2GM}{b}w\right)^{1/2}\right]^{-1/2} \tag{51}$$

where we have set $w = \frac{b}{r}$ and $a = \frac{\tilde{A}_0 b}{J}$.
If we expand the integral in powers of $\frac{2GM}{b}$ and a we find:

$$\Delta\phi_{SFR} \approx 2\int_{0}^{w_1} dw\frac{1 + \frac{GM}{b}w}{\left[(1-2a) + \frac{2GM}{b}w - w^2\right]^{1/2}} \tag{52}$$

where we have omitted second order terms.
By evaluating the integral in Eq. (52) we get (see Appendix 3):

$$\Delta\phi_{SFR} = \pi + \frac{4GM}{b}\frac{1-a}{\sqrt{1-2a}} \tag{53}$$

The deflection angle $\delta\phi_{SFR}$ can be found as:

$$\delta\phi_{SFR} = \Delta\phi_{SFR} - \pi \Rightarrow$$

$$\delta\phi_{SFR} = \frac{4GM}{b}\frac{1-a}{\sqrt{1-2a}} \tag{54}$$

If we expand Eq. (54) in powers of $a = \frac{\tilde{A}_0 b}{J}$ the deflection angle can be written as:

$$\delta\phi_{SFR} \approx \left(1 + \frac{a^2}{2}\right)\frac{4GM}{b} \tag{55}$$

The deflection angle $\delta\phi$ of GR [3, 68] is given by:

$$\delta\phi_{GR} = \frac{4GM}{b} \tag{56}$$

Therefore, we notice that the deflection angle of SFR includes a small additional Randers contribution term a which shows a small deviation from GR because $|\tilde{A}_0| \ll 1$. We can see from Eq. (54) that:

$$\lim_{\tilde{A}_0 \to 0} \delta\phi_{SFR} = \delta\phi_{GR} \tag{57}$$

The small difference of the deflection angle of the SFR model from the GR one can plausibly be attributed to the Lorentz violations [6] or on the small amount of energy which is added to the gravitational potential of SFR.

Remark: By considering the following relation, we can connect the geometrical concept of the curvature $\kappa_\phi = \frac{d\phi}{d\tau}$ of a path with the deflection angle $\delta\phi$ in the following way:

$$\dot{\phi} = \frac{d\phi}{d\tau} = \frac{d\phi}{dr}\frac{dr}{d\tau} = \frac{d\phi}{dr}\dot{r} \Rightarrow \tag{58}$$

$$\kappa_\phi = \frac{d\phi}{dr}\dot{r} \Rightarrow \tag{59}$$

$$\delta\phi = \int \frac{\kappa_\phi}{\dot{r}} dr \tag{60}$$

This form of curvature can be called *deflection curvature*.

VI. CONCLUSIONS & FUTURE CHALLENGES

In this article, we investigated the analytic form of the geodesics of the model SFR which was introduced in previous works [1, 2]. A dynamical analysis was presented based on the energy and angular momentum of a particle along of geodesics (null or timelike) of the SFR spacetime. Comparisons between the SFR and GR were provided. We found that there is a small deviation from the GR model which is due to the dynamical term $A_\gamma(x)$. We also formulated and studied an effective potential of our model and we compared the one of the SFR case once again with the effective potential of GR attributing the small but discernible differences to the specific structure of (and perturbation incorporated within) the SFR spacetime. The relevant differences in the trajectories were illustrated both in the evolution over the time-variable τ and in the (x, y) plane. In addition, we calculated the deflection angle for the SFR spacetime and we compared with the corresponding one of GR. The result is a small difference of the SFR model from GR, it is possibly caused by Lorentz violations or by the small amount of energy which is added to the gravitational potential of SFR spacetime.

It is important to note that this work opens a number of interesting directions of further study for the future. On the one hand, the traditional assumption of $\theta = \pi/2$ made over here is clearly a restrictive one that simplifies the equations of motion automatically satisfying the dynamics for the angular variable θ with the latter being at steady state. However, more generally, one can straightforwardly envision scenarios where this condition is no longer satisfied. It is then of interest to explore if one starts in the vicinity of $\pi/2$ whether one stays in that neighborhood or perhaps if one deviates away from this steady state and how the associated dynamics of the full 4-degree-of-freedom space is accordingly explored. Another aspect that is also worth further exploring is that of the small amplitude covector deviation from the General Relativity standard model. Here, we have limited our considerations to the realm of associated small amplitude perturbations (where leading order expansions of the field would suffice). However, it would also be of interest to explore the situation when one gradually deviates from the realm of this approximation as well. In addition, applications of geodesics of the SFR model can be pursued for more concrete cosmological studies such as, e.g., for the case of the S2 stars orbiting the black hole in Sagittarius A* in which the geodesics of the star are perturbed from the classical Keplerian orbits because of the distribution of stellar remnants. Indeed, our hope is that this work may pave the way towards testing the Schwarzschild-Finsler-Randers gravitational model which incorporates features going beyond the standard Riemannian geometry of spacetime. In this vein, some of the above topics are presently under consideration and associated results will be presented in future publications.

VII. ACKNOWLEDGEMENTS

The authors would like to thank Gary Gibbons for his valuable suggestions.

Appendix A: Distinguished connection on TM.

In this work, we consider a distinguished connection ($d-$connection) D on TM [66, 67]. This is a linear connection with coefficients $\{\Gamma^A_{BC}\} = \{L^\mu_{\nu\kappa}, L^\alpha_{\beta\kappa}, C^\mu_{\nu\gamma}, C^\alpha_{\beta\gamma}\}$ which preserves by parallelism the horizontal and vertical distributions:

$$D_{\delta_\kappa}\delta_\nu = L^\mu_{\nu\kappa}(x,y)\delta_\mu \quad , \quad D_{\dot{\partial}_\gamma}\delta_\nu = C^\mu_{\nu\gamma}(x,y)\delta_\mu \tag{A1}$$

$$D_{\delta_\kappa}\dot{\partial}_\beta = L^\alpha_{\beta\kappa}(x,y)\dot{\partial}_\alpha \quad , \quad D_{\dot{\partial}_\gamma}\dot{\partial}_\beta = C^\alpha_{\beta\gamma}(x,y)\dot{\partial}_\alpha \tag{A2}$$

From the above conditions, the definitions for partial covariant differentiation follow immediately, e.g. for $X \in TTM$ the expression for the covariant h-derivative is:

$$X^A_{|\nu} \equiv D_\nu\, X^A \equiv \delta_\nu X^A + L^A_{B\nu}X^B \tag{A3}$$

and for the covariant v-derivative:

$$X^A|_\beta \equiv D_\beta\, X^A \equiv \dot{\partial}_\beta X^A + C^A_{B\beta}X^B \tag{A4}$$

The $d-$connection is metric-compatible when we have:

$$D_\kappa\, g_{\mu\nu} = 0, \quad D_\kappa\, v_{\alpha\beta} = 0, \quad D_\gamma\, g_{\mu\nu} = 0, \quad D_\gamma\, v_{\alpha\beta} = 0 \tag{A5}$$

A $d-$connection can be uniquely defined when the following conditions are satisfied:

- The $d-$connection is metric compatible

- Coefficients $L^{\mu}_{\nu\kappa}, L^{\alpha}_{\beta\kappa}, C^{\mu}_{\nu\gamma}, C^{\alpha}_{\beta\gamma}$ depend solely on the quantities $g_{\mu\nu}$, $v_{\alpha\beta}$ and N^{α}_{μ}
- Coefficients $L^{\mu}_{\kappa\nu}$ and $C^{\alpha}_{\beta\gamma}$ are symmetric on the lower indices, i.e. $L^{\mu}_{[\kappa\nu]} = C^{\alpha}_{[\beta\gamma]} = 0$

We use the symbol $\mathcal{D}$ instead of D for a connection satisfying these conditions. We call $\mathcal{D}$ a canonical and distinguished $d-$connection. The coefficients of this connection are

$$L^{\mu}_{\nu\kappa} = \frac{1}{2} g^{\mu\rho} \left(\delta_k g_{\rho\nu} + \delta_\nu g_{\rho\kappa} - \delta_\rho g_{\nu\kappa} \right) \tag{A6}$$

$$L^{\alpha}_{\beta\kappa} = \dot{\partial}_\beta N^{\alpha}_{\kappa} + \frac{1}{2} v^{\alpha\gamma} \left(\delta_\kappa v_{\beta\gamma} - v_{\delta\gamma}\, \dot{\partial}_\beta N^{\delta}_{\kappa} - v_{\beta\delta}\, \dot{\partial}_\gamma N^{\delta}_{\kappa} \right) \tag{A7}$$

$$C^{\mu}_{\nu\gamma} = \frac{1}{2} g^{\mu\rho} \dot{\partial}_\gamma g_{\rho\nu} \tag{A8}$$

$$C^{\alpha}_{\beta\gamma} = \frac{1}{2} v^{\alpha\delta} \left(\dot{\partial}_\gamma v_{\delta\beta} + \dot{\partial}_\beta v_{\delta\gamma} - \dot{\partial}_\delta v_{\beta\gamma} \right) \tag{A9}$$

Curvatures and torsions on TM are defined by the linear maps:

$$\mathcal{R}(X,Y)Z = [\mathcal{D}_X, \mathcal{D}_Y]Z - \mathcal{D}_{[X,Y]}Z \tag{A10}$$

and

$$\mathcal{T}(X,Y) = \mathcal{D}_X Y - \mathcal{D}_Y X - [X,Y] \tag{A11}$$

where $X, Y, Z \in TTM$. We use the following definitions for the curvature components [66, 67]:

$$\mathcal{R}(\delta_\lambda, \delta_\kappa)\delta_\nu = R^{\mu}_{\nu\kappa\lambda}\delta_\mu \tag{A12}$$

$$\mathcal{R}(\delta_\lambda, \delta_\kappa)\dot{\partial}_\beta = R^{\alpha}_{\beta\kappa\lambda}\dot{\partial}_\alpha \tag{A13}$$

$$\mathcal{R}(\dot{\partial}_\gamma, \delta_\kappa)\delta_\nu = P^{\mu}_{\nu\kappa\gamma}\delta_\mu \tag{A14}$$

$$\mathcal{R}(\dot{\partial}_\gamma, \delta_\kappa)\dot{\partial}_\beta = P^{\alpha}_{\beta\kappa\gamma}\dot{\partial}_\alpha \tag{A15}$$

$$\mathcal{R}(\dot{\partial}_\delta, \dot{\partial}_\gamma)\delta_\nu = S^{\mu}_{\nu\gamma\delta}\delta_\mu \tag{A16}$$

$$\mathcal{R}(\dot{\partial}_\delta, \dot{\partial}_\gamma)\dot{\partial}_\beta = S^{\alpha}_{\beta\gamma\delta}\dot{\partial}_\alpha \tag{A17}$$

In addition, we use the following definitions for the torsion components:

$$\mathcal{T}(\delta_\kappa, \delta_\nu) = \mathcal{T}^{\mu}_{\nu\kappa}\delta_\mu + \mathcal{T}^{\alpha}_{\nu\kappa}\dot{\partial}_\alpha \tag{A18}$$

$$\mathcal{T}(\dot{\partial}_\beta, \delta_\nu) = \mathcal{T}^{\mu}_{\nu\beta}\delta_\mu + \mathcal{T}^{\alpha}_{\nu\beta}\dot{\partial}_\alpha \tag{A19}$$

$$\mathcal{T}(\dot{\partial}_\gamma, \dot{\partial}_\beta) = \mathcal{T}^{\mu}_{\beta\gamma}\delta_\mu + \mathcal{T}^{\alpha}_{\beta\gamma}\dot{\partial}_\alpha \tag{A20}$$

From (A12), the h-curvature tensor of the $d-$connection in the adapted basis and the corresponding h-Ricci tensor read:

$$R^{\mu}_{\nu\kappa\lambda} = \delta_\lambda L^{\mu}_{\nu\kappa} - \delta_\kappa L^{\mu}_{\nu\lambda} + L^{\rho}_{\nu\kappa} L^{\mu}_{\rho\lambda} - L^{\rho}_{\nu\lambda} L^{\mu}_{\rho\kappa} + C^{\mu}_{\nu\alpha}\Omega^{\alpha}_{\kappa\lambda} \tag{A21}$$

$$R_{\mu\nu} = R^{\kappa}_{\mu\nu\kappa} = \delta_\kappa L^{\kappa}_{\mu\nu} - \delta_\nu L^{\kappa}_{\mu\kappa} + L^{\rho}_{\mu\nu} L^{\kappa}_{\rho\kappa} - L^{\rho}_{\mu\kappa} L^{\kappa}_{\rho\nu} + C^{\kappa}_{\mu\alpha}\Omega^{\alpha}_{\nu\kappa} \tag{A22}$$

From (A17), the v-curvature tensor of the d−connection in the adapted basis and the corresponding v-Ricci tensor are:

$$S^{\alpha}_{\beta\gamma\delta} = \dot{\partial}_{\delta} C^{\alpha}_{\beta\gamma} - \dot{\partial}_{\gamma} C^{\alpha}_{\beta\delta} + C^{\epsilon}_{\beta\gamma} C^{\alpha}_{\epsilon\delta} - C^{\epsilon}_{\beta\delta} C^{\alpha}_{\epsilon\gamma} \tag{A23}$$

$$S_{\alpha\beta} = S^{\gamma}_{\alpha\beta\gamma} = \dot{\partial}_{\gamma} C^{\gamma}_{\alpha\beta} - \dot{\partial}_{\beta} C^{\gamma}_{\alpha\gamma} + C^{\epsilon}_{\alpha\beta} C^{\gamma}_{\epsilon\gamma} - C^{\epsilon}_{\alpha\gamma} C^{\gamma}_{\epsilon\beta} \tag{A24}$$

The generalized Ricci scalar curvature in the adapted basis is:

$$\mathcal{R} = g^{\mu\nu} R_{\mu\nu} + v^{\alpha\beta} S_{\alpha\beta} = R + S \tag{A25}$$

where

$$R = g^{\mu\nu} R_{\mu\nu} \quad , \quad S = v^{\alpha\beta} S_{\alpha\beta} \tag{A26}$$

Appendix B: Field equations of the model.

A Hilbert-like action on TM can be defined as

$$K = \int_{\mathcal{N}} d^8\mathcal{U} \sqrt{|\mathcal{G}|}\, \mathcal{R} + 2\kappa \int_{\mathcal{N}} d^8\mathcal{U} \sqrt{|\mathcal{G}|}\, \mathcal{L}_M \tag{B1}$$

for some closed subspace $\mathcal{N} \subset TM$, where $|\mathcal{G}|$ is the absolute value of the metric determinant, $\mathcal{L}_M$ is the Lagrangian of the matter fields, κ is a constant and

$$d^8\mathcal{U} = \mathrm{d}x^0 \wedge \ldots \wedge \mathrm{d}x^3 \wedge \mathrm{d}y^4 \wedge \ldots \wedge \mathrm{d}y^7 \tag{B2}$$

Variation with respect to $g_{\mu\nu}$, $v_{\alpha\beta}$ and N^{α}_{κ} leads to the following field equations [38]:

$$\overline{R}_{\mu\nu} - \frac{1}{2}(R+S)\, g_{\mu\nu} + \left(\delta^{(\lambda}_{\nu}\delta^{\kappa)}_{\mu} - g^{\kappa\lambda} g_{\mu\nu}\right)\left(\mathcal{D}_{\kappa} \mathcal{T}^{\beta}_{\lambda\beta} - \mathcal{T}^{\gamma}_{\kappa\gamma} \mathcal{T}^{\beta}_{\lambda\beta}\right) = T_{\mu\nu} \tag{B3}$$

$$S_{\alpha\beta} - \frac{1}{2}(R+S)\, v_{\alpha\beta} + \left(v^{\gamma\delta} v_{\alpha\beta} - \delta^{(\gamma}_{\alpha}\delta^{\delta)}_{\beta}\right)\left(\mathcal{D}_{\gamma} C^{\mu}_{\mu\delta} - C^{\nu}_{\nu\gamma} C^{\mu}_{\mu\delta}\right) = Y_{\alpha\beta} \tag{B4}$$

$$g^{\mu[\kappa} \dot{\partial}_{\alpha} L^{\nu]}_{\mu\nu} + 2\mathcal{T}^{\beta}_{\mu\beta} g^{\mu[\kappa} C^{\lambda]}_{\lambda\alpha} = \mathcal{Z}^{\kappa}_{\alpha} \tag{B5}$$

where

$$\mathcal{T}^{\alpha}_{\nu\beta} = \dot{\partial}_{\beta} N^{\alpha}_{\nu} - L^{\alpha}_{\beta\nu} \tag{B6}$$

are torsion components, where $L^{\alpha}_{\beta\nu}$ is defined in (19). From the form of (8) it follows that $\sqrt{|\mathcal{G}|} = \sqrt{-g}\sqrt{-v}$, with g, v the determinants of the metrics $g_{\mu\nu}, v_{\alpha\beta}$ respectively.

Appendix C: Calculation of the deflection angle

We begin the calculation from Eq. (51)

$$\Delta\phi_{SFR} = 2\int_0^{w_1} dw \left[1 - w^2\left(1 - \frac{2GM}{b} w\right) - 2a\left(1 - \frac{2GM}{b} w\right)^{1/2}\right]^{-1/2} \tag{C1}$$

$$\Delta\phi_{SFR} = 2\int_0^{w_1} dw \left(1-\frac{2GM}{b}w\right)^{-1/2}\left[\left(1-\frac{2GM}{b}w\right)^{-1} - w^2 - 2a\left(1-\frac{2GM}{b}w\right)^{-1/2}\right]^{-1/2} \Rightarrow$$

$$\Delta\phi_{SFR} \approx 2\int_0^{w_1} dw \left(1+\frac{GM}{b}w\right)\left[\left(1+\frac{2GM}{b}w\right) - w^2 - 2a\right]^{-1/2} \Rightarrow$$

$$\Delta\phi_{SFR} \approx 2\int_0^{w_1} dw \frac{1+\frac{GM}{b}w}{\left[\left(1+\frac{2GM}{b}w\right) - w^2 - 2a\right]^{1/2}} \Rightarrow$$

$$\Delta\phi_{SFR} \approx 2\int_0^{w_1} dw \frac{1+\frac{GM}{b}w}{\left[(1-2a)+\frac{2GM}{b}w - w^2\right]^{1/2}} \tag{C2}$$

In order to find w_1 we solve the following equation from the denominator:

$$(1-2a)+\frac{2GM}{b}w - w^2 = 0 \tag{C3}$$

and we get:

$$w_1 = \frac{GM}{b} + \sqrt{\left(\frac{GM}{b}\right)^2 + (1-2a)} \tag{C4}$$

which is the positive root of the denominator. The solution for the integral in Eq. (C2) is:

$$\Delta\phi_{SFR} = \pi + \frac{1}{\sqrt{1-2a}}\frac{2GM}{b} + \frac{2GM}{b}\sqrt{1-2a} \tag{C5}$$

where we omit terms $O((\frac{2GM}{b})^2)$, given their smallness. Hence, we find:

$$\Delta\phi_{SFR} = \pi + \frac{4GM}{b}\frac{1-a}{\sqrt{1-2a}} \tag{C6}$$

[1] A. Triantafyllopoulos, S. Basilakos, E. Kapsabelis and P. C. Stavrinos, *Schwarzschild-like solutions in Finsler–Randers gravity,* Eur. Phys. J. C **80** (2020) no.12, 1200
[2] E. Kapsabelis, A. Triantafyllopoulos, S. Basilakos and P. C. Stavrinos, *Applications of the Schwarzschild–Finsler–Randers model,* Eur. Phys. J. C **81** (2021) no.11, 990
[3] J. Hartle, *Gravity: An Introduction to Einstein's General Relativity.* Pearson Education Inc, Addison Wesley: San Francisco (2002)
[4] G. S. Asanov and P. C. Stavrinos, *Finslerian deviations of Geodesics over tangent bundle,* Reports on Mathematical Physics **30**, no.1 (1991) 63–69
[5] P. C. Stavrinos and S. Ikeda, *Some connections and variational principle to the Finslerian scalar-tensor theory of gravitation,* Reports on Mathematical Physics **44** no.1–2 (1999) 221–230
[6] V. A. Kostelecký, *Riemann-Finsler geometry and Lorentz-violating kinematics,* Phys. Lett. B **701** (2011) 137
[7] V. Alan Kostelecký, N. Russell and R. Tso, *Bipartite Riemann–Finsler geometry and Lorentz violation,* Phys. Lett. B **716** (2012) 470–474
[8] P. Stavrinos, *Weak Gravitational Field in Finsler-Randers Space and Raychaudhuri Equation,* Gen. Rel. Grav. **44** (2012) 3029–3045

[9] E. Minguzzi, *Raychaudhuri equation and singularity theorems in Finsler spacetimes,* Class. Quant. Grav. **32** (2015) no.18, 185008

[10] J. Foster and R. Lehnert, *Classical-physics applications for Finsler b space,* Phys. Lett. B **746** (2015) 164

[11] V. Antonelli, L. Miramonti and M. D. C. Torri, *Neutrino oscillations and Lorentz Invariance Violation in a Finslerian Geometrical model,* Eur. Phys. J. C **78** (2018) no.8, 667

[12] B. R. Edwards and V. A. Kostelecký, *Riemann–Finsler geometry and Lorentz-violating scalar fields,* Phys. Lett. B **786** (2018) 319-326

[13] S. Ikeda, E. N. Saridakis, P. C. Stavrinos and A. Triantafyllopoulos, *Cosmology of Lorentz fiber-bundle induced scalar-tensor theories,* Phys. Rev. D **100** (2019) no.12, 124035

[14] J. J. Relancio and S. Liberati, *Constraints on the deformation scale of a geometry in the cotangent bundle,* Phys. Rev. D **102** (2020) no.10, 104025

[15] P. Stavrinos and C. Savvopoulos, *Dark Gravitational Field on Riemannian and Sasaki Spacetime,* Universe **6** (2020) no.9, 138

[16] A. P. Kouretsis, M. Stathakopoulos and P. C. Stavrinos, *The General Very Special Relativity in Finsler Cosmology,* Phys. Rev. D **79** (2009) 104011

[17] N. E. Mavromatos, S. Sarkar and A. Vergou, *Stringy Space-Time Foam, Finsler-like Metrics and Dark Matter Relics,* Phys. Lett. B **696** (2011) 300

[18] P. Stavrinos and S. I. Vacaru, *Broken Scale Invariance, Gravity Mass, and Dark Energy in Modified Einstein Gravity with Two Measure Finsler Like Variables,* Universe **7** (2021) no.4, 89

[19] S. Konitopoulos, E. N. Saridakis, P. C. Stavrinos and A. Triantafyllopoulos, *Dark gravitational sectors on a generalized scalar-tensor vector bundle model and cosmological applications,* Phys. Rev. D **104** (2021) no.6, 064018

[20] R. Hama, T. Harko and S. V. Sabau, *Dark energy and accelerating cosmological evolution from osculating Barthel–Kropina geometry,* Eur. Phys. J. C **82** (2022) no.4, 385

[21] G. W. Gibbons, J. Gomis and C. N. Pope, *General very special relativity is Finsler geometry,* Phys. Rev. D **76** (2007) 081701

[22] J. Skakala and M. Visser, *Bi-metric pseudo-Finslerian spacetimes,* J. Geom. Phys. **61** (2011) 1396–1400

[23] R. Gallego Torrome, P. Piccione and H. Vitorio, *On Fermat's principle for causal curves in time oriented Finsler spacetimes,* J. Math. Phys. **53** (2012), 123511

[24] P. Stavrinos, O. Vacaru and S. I. Vacaru, *Modified Einstein and Finsler like theories on tangent Lorentz bundles,* Int. J. Mod. Phys. D **23** (2014) no.11, 1450094

[25] A. Fuster and C. Pabst, *Finsler pp-waves,* Phys. Rev. D **94** (2016) no.10, 104072

[26] N. Voicu, *Volume forms for time orientable Finsler spacetimes,* J. Geom. Phys. **112** (2017), 85-94

[27] M. Hohmann, C. Pfeifer and N. Voicu, *Finsler gravity action from variational completion,* Phys. Rev. D **100** (2019) no.6, 064035

[28] D. Colladay and L. Law, *Spontaneous CPT breaking and fermion propagation in the Schwarzschild geometry,* Phys. Lett. B **795** (2019) 457–461

[29] E. Caponio and A. Masiello, *On the analyticity of static solutions of a field equation in Finsler gravity,* Universe **6** (2020) no.4, 59

[30] R. Hama, T. Harko, S. V. Sabau and S. Shahidi, *Cosmological evolution and dark energy in osculating Barthel-Randers geometry,* Eur. Phys. J. C **81** (2021) 742

[31] G. Randers, *On an Asymmetrical Metric in the Four-Space of General Relativity,* Phys. Rev. **59** (1941) no.2, 195–199

[32] J. I. Horváth, *A Geometrical Model for the Unified Theory of Physical Fields,* Phys. Rev. **80** (1950) 901

[33] J. I. Horváth, A. Moór, *Entwicklung einer einheitlichen Feldtheorie begründet auf die Finslersche Geometrie,* Z. Physik **131** (1952) 544–570

[34] Y. Takano, *Theory of Fields in Finsler Spaces. I,* Prog. Theor. Phys. **40** (1968) no.5, Pages 1159—1180

[35] S. Ikeda, *On the theory of fields in Finsler spaces,* J. Math. Phys. **22** (1981) 1215

[36] G. S. Asanov, *Gravitational field equations based on Finsler geometry,* Foundations of Physics **13** (1983) no.5, 501–527

[37] A. Triantafyllopoulos and P. C. Stavrinos, *Weak field equations and generalized FRW cosmology on the tangent Lorentz bundle,* Class. Quant. Grav. **35** (2018) no.8, 085011

[38] A. Triantafyllopoulos, E. Kapsabelis and P. C. Stavrinos, *Gravitational Field on the Lorentz Tangent Bundle: Generalized Paths and Field Equations,* Eur. Phys. J. Plus **135** (2020) no.7, 557

[39] P. C. Stavrinos, *Congruences of Fluids in a Finslerian Anisotropic Space-Time,* Int. J. Theor. Phys. **44**, 245-–254 (2005)

[40] P. C. Stavrinos, A. P. Kouretsis and M. Stathakopoulos, *Friedmann Robertson-Walker model in generalised metric space-time with weak anisotropy,* Gen. Rel. Grav. **40**, 1403–1425 (2008)
[41] F. Girelli, S. Liberati and L. Sindoni, *Planck-scale modified dispersion relations and Finsler geometry,* Phys. Rev. D **75** (2007) 064015
[42] E. Minguzzi, *Light cones in Finsler spacetime,* Commun. Math. Phys. **334** (2015) no.3, 1529-1551
[43] M. A. Javaloyes and M. Sánchez, *On the definition and examples of cones and Finsler spacetimes,* RACSAM **114** (2019) No.1, 30
[44] J. E. G. Silva and C. A. S. Almeida, *Kinematics and dynamics in a Bipartite-Finsler spacetime,* Phys. Lett. B **731** (2014) 74–79
[45] V. A. Kostelecký and M. Mewes, *Astrophysical Tests of Lorentz and CPT Violation with Photons,* Astrophys. J. **689** (2008) L1
[46] S. I. Vacaru, *Principles of Einstein-Finsler Gravity and Perspectives in Modern Cosmology,* Int. J. Mod. Phys. D **21** (2012) 1250072
[47] P. C. Stavrinos and S. I. Vacaru, *Cyclic and Ekpyrotic Universes in Modified Finsler Osculating Gravity on Tangent Lorentz Bundles,* Class. Quant. Grav. **30** (2013) 055012
[48] M. Hohmann and C. Pfeifer, *Geodesics and the magnitude-redshift relation on cosmologically symmetric Finsler spacetimes,* Phys. Rev. D **95** (2017) no. 10, 104021
[49] D. C. Brody, G. W. Gibbons and D. M. Meier, *A Riemannian approach to Randers geodesics,* J. Geom. Phys. **106** (2016) 98–101
[50] S. Chanda, G. W. Gibbons, P. Guha, P. Maraner and M. C. Werner, *Jacobi-Maupertuis Randers-Finsler metric for curved spaces and the gravitational magnetoelectric effect,* J. Math. Phys. **60** (2019) no.12, 122501
[51] S. Chanda and P. Guha, *Eisenhart lift and Randers–Finsler formulation for scalar field theory,* Eur. Phys. J. Plus **136** (2021) no.1, 66
[52] S. Heefer, C. Pfeifer and A. Fuster, *Randers pp-waves,* Phys. Rev. D **104** (2021) no.2, 024007
[53] H. Lou, J. Li, W. Yang, W. Feng, W. Liu, Q. Zhang, N. Zhang, Y. Qi and Y. Wu, *Theoretical analysis on the Rényi holographic dark energy in the Finsler–Randers cosmology,* Int. J. Mod. Phys. D **31** (2022) no.02, 2250002
[54] S. Angit, R. Raushan and R. Chaubey, *Stability and bifurcation analysis of Finsler–Randers cosmological model,* Pramana **96** (2022) no.3, 123. Indian Academy of Sciences
[55] P. C. Stavrinos and F. I. Diakogiannis, *A Geometric anisotropic model of space-time based on Finslerian metric,* Gravitation and Cosmology **10** (2004) 269–278
[56] Z. Chang and X. Li, *Lorentz invariance violation and symmetry in Randers-Finsler spaces,* Phys. Lett. B **663** (2008) 103
[57] S. Basilakos, A. P. Kouretsis, E. N. Saridakis and P. Stavrinos, *Resembling dark energy and modified gravity with Finsler-Randers cosmology,* Phys. Rev. D **88** (2013) 123510
[58] S. Basilakos and P. Stavrinos, *Cosmological equivalence between the Finsler-Randers space-time and the DGP gravity model,* Phys. Rev. D **87** (2013) no. 4, 043506
[59] P. C. Stavrinos and M. Alexiou, *Raychaudhuri equation in the Finsler–Randers space-time and generalized scalar-tensor theories,* Int. J. Geom. Meth. Mod. Phys. **15**, no.03, 1850039 (2017)
[60] G. Papagiannopoulos, S. Basilakos, A. Paliathanasis, S. Savvidou and P. C. Stavrinos, *Finsler–Randers cosmology: dynamical analysis and growth of matter perturbations,* Class. Quant. Grav. **34** (2017) no.22, 225008
[61] J. E. G. Silva, R. V. Maluf and C. A. S. Almeida, *A nonlinear dynamics for the scalar field in Randers spacetime*, Phys. Lett. B **766** (2017) 263–267
[62] R. Chaubey, B. Tiwari, A. Shukla and M. Kumar, *Finsler–Randers Cosmological Models in Modified Gravity Theories,* Proc. Nat. Inst. Sci. India (Pt. A Phys. Sci.) **89** (2019) no.4, 757–768
[63] R. Raushan and R. Chaubey, *Finsler–Randers cosmology in the framework of a particle creation mechanism: a dynamical systems perspective,* Eur. Phys. J. Plus **135** (2020) no.2, 228
[64] G. Papagiannopoulos, S. Basilakos, A. Paliathanasis, S. Pan and P. Stavrinos, *Dynamics in varying vacuum Finsler–Randers cosmology,* Eur. Phys. J. C **80** (2020) no.9, 816
[65] J. E. G. Silva, *A field theory in Randers-Finsler spacetime,* EPL **133** (2021) no.2, 21002
[66] R. Miron and M. Anastasiei, *The Geometry of Lagrange Spaces: Theory and Applications,* Fundam. Theor. Phys. , Springer Netherlands, Dordrecht (1994)
[67] S. Vacaru, P. C. Stavrinos, E. Gaburov and D. Gonta, *Clifford and Riemann-Finsler structures in geometric mechanics and gravity,* Differential Geometry – Dynamical Systems, Monograph 7, Geometry Balkan Press, Bucharest (2006)

[68] S. Carroll, *Spacetime and Geometry, An Introduction to General Relativity,* Pearson Education Inc, Addison Wesley (2004)